Archives of Microbiology (2025) 207:138
https://doi.org/10.1007/s00203-025-04345-9

ORIGINAL PAPER

Molecular and functional analysis of a putative pyocin S9, with endonuclease activity from *P. chlororaphis* subsp *aurantiaca* PB-St2

Maryam Zareen[1] · Deeba Noreen Baig[1] · Muhammad Imran[1] · Zabish Khaliq[1] · Kausar Abdulla Malik[1] · Andreas Bechthold[2] · Samina Mehnaz[1]

Received: 5 March 2025 / Revised: 16 April 2025 / Accepted: 26 April 2025

Abstract
Pyocins are bacteriocins which are explicitly associated with pseudomonads. In this study, the genome mining and in-depth sequence analysis identified three similar S9-like (a, b, and c), an S3-like (d) and one R-type pyocin systems from *P. chlororaphis* subsp *aurantiaca* PB-St2. The phenotypic screening of bacteriocin production by PB-St2 indicated narrow-spectrum bactericidal activity against closely related *Pseudomonas* species i.e., *Pseudomonas aeruginosa* PAi, PAc1, PAc3, PAc4; *Pseudomonas fluorescens* Psi-RS1 and *Pseudomonas kilonensis* OSRS3. Herein, the proposed pyocin S9c was further selected for molecular and functional characterization. The presumptive N-terminal receptor binding domain of candidate system lacks significant similarity with any characterized HNH-type pyocin S DN*ases* from *P. aeruginosa.* In contrast, the cytotoxic domain showed 53% sequence similarity with pyocin S8 and 70% to pyocin S9. Thus, pyocin S9c was suggested as an isoform under the Class I DN*ase* (H-N-H) family in pyocin S9 cluster, commonly found in *P. chlororaphis* subsp. *aurantiaca* and *P. chlororaphis* subsp *aureofaciens* strains. Molecular screening of the pyocin S9c system revealed its presence in 6 out of 7 tested strains of *P. chlororaphis* subsp. *aurantiaca* GS1, GS3, GS4, GS6, ARS38, FS2 and one *P. chlororaphis* RP4 relative strains, isolated from diverse plant hosts. The 1.59 kb fragment consisting of two structural genes of pyocin-immunity operon (S9c) in *P. aurantiaca* PB-St2 were cloned in *pET28a*(+) and expressed in *Escherichia coli* BL21 DE3 (pLysS) strain as a fusion protein with histidine tag. The recombinant cytotoxic protein of pyocin S9c operon was purified with N-term His-tag with a molecular weight of ≈50 kDa. The identity of target protein was affirmed by tandem mass spectrometry analysis. The purified cytotoxic protein was active against *P. chlororaphis* subsp. *aurantiaca* GS7, with a minimum inhibitory concentration of 12.5 µg/ml. The mechanism of cytotoxicity was affirmed as a metal-dependent endonuclease by evidence of non-specific hydrolysis of pTZ57R plasmid isoforms. These results indicate that pyocin S9c can contribute to the rhizo-competence of this strain in plant-associated natural habitats, occupied by related *Pseudomonas* strains.

Keywords *Pseudomonas aurantiaca* · S-type pyocin · Cytotoxic protein S9c · Immunity protein Im9c · Heterologous protein expression · Endonuclease activity

Introduction

In nature, microbial antagonism is the ability of microbes to compete among themselves for food and shelter. Micro-organisms containing antimicrobial lytic enzymes and metabolites serve as a diverse reservoir of bioactive natural products. A deep insight into their occurrence, biosynthesis, and mechanism of action not only adds to our understanding of microbial defense but also facilitates in assessing their potential as a biotechnological product.

Pseudomonas chlororaphis, a gram-negative γ-proteobacterium is classified as a phylogroup in

Communicated by PANKAJ BHATT

✉ Samina Mehnaz
saminamehnaz@fccollege.edu.pk

1 KAM School of Life Sciences, Forman Christian College (A Chartered University), Ferozepur Road, Lahore 54600, Pakistan

2 Department of Pharmaceutical Biology and Biotechnology, Albert-Ludwigs- Universitat Freiburg, Freiburg 79104, Germany

Published online: 08 May 2025

Pseudomonas fluorescens complex (Garrido-Sanz et al. 2017). Based on differences in fatty acid profile and phenotypic traits, *P. aurantiaca* had been proposed as a subspecie of *P. chlororaphis* i.e., *P. chlororaphis* subsp *aurantiaca* (Peix et al. 2007). Numerous strains of *P. chlororaphis* subsp *aurantiaca* had been isolated around the world from various plant hosts. With a history of safe usage, this subspecie has emerged as a biotechnological asset with promising eco-physiological traits such as bioremediation of polluted environments (Khaled Abd El-Aziz et al. 2016), plant health protection (Jiao et al. 2013; Hou et al. 2025) and growth stimulation (Rosas et al. 2009; Fang et al. 2013; Shahid et al. 2017; Abbas et al. 2024). The biocontrol ability of this subspecie is associated with production of vast array of diverse secondary metabolites such as phenazine derivatives PCA, 2-OH-PHZ (Mehnaz et al. 2009; Zhang et al. 2022), pyrrolnitrin, siderophores (Shahid et al. 2021), 2-hexyl, 5-propyl resorcinol HPR (Nowak-Thompson et al. 2003), rhamnolipids, hydrogen cyanide, lippopeptides, lytic exozymes and associated regulatory quorum sensing system (Morohoshi et al. 2013; Bauer et al. 2016).

In addition to bioactive secondary metabolites, bacterial antagonism is linked with the production of bacteriocins, contact-dependent inhibitory (CDI) proteins, and type-VI-secreted determinants. Bacteriocins are a highly diverse group of ribosomally synthesized antimicrobial peptides and proteins. These are contact-independent effector proteins, mostly produced in the primary bacterial growth phase with or without stress induction. Their extracellular release is often mediated through cellular lysis. Historically, the first bacteriocin identified in *P. aeruginosa* was called pyocin (Jacob 1954). So far, four types of pyocins have been characterized in different strains of *P. aeruginosa*. R-type and F-type tailocins, L-type (lectin-like) and S-type soluble pyocins (Ghequire and De-Mot 2014, 2015). S-type pyocins are colicin-like, low molecular weight, protease-sensitive secretory antibacterial proteins (Briand and Baysse 2002). Unlike colicins that are plasmid borne, the genetic counterparts of pyocin S are located on the chromosome and known to possess species-specific bactericidal activity. Pyocin-producing bacteria codes for two different polypeptides in the same operon forming a complex. First protein is the cytotoxic protein, which is larger in the molecular mass followed by a relatively small immunity protein. The co-expression of this membrane-localized immunity protein prevents the self-intoxication of producing cells. The Pyocin S proteins are reported as functional DN*ases*, RN*ases*, pore-formers or inhibitors of lipid synthesis in the susceptible host cell. The nuclease type pyocin S is further classified into several subtypes (S1, S2, S3, S5, S6, S8, S9 and AP41) based on sequence and antibacterial spectrum diversity (Sano and Kageyama 1981; Sano et al. 1993; Duport et al. 1995; Ling et al. 2010; Dingemans et al. 2016; Turano et al. 2020). The C-terminal of the DNase-type I cytotoxic protein houses a conserved catalytic core i.e., an H-N-H motif expressing endonuclease activity. This motif coordinates a single divalent metal ion for performing random cleavage of the bacterial genome (Sano 1993; Briand and Baysse 2002; Turano et al. 2020).

Until now, most studies regarding S-type pyocins have been conducted exclusively on *P. aeruginosa* strains reporting several sub-classes. However, in-silico analysis of publicly available genomes predicted widespread and novel occurrences of these antimicrobials among diverse species of pseudomonads (Ghequire and De Mot 2014). Although, *P. chlororaphis* species has been widely studied for its huge capacity to produce biologically active secondary metabolites, however, not much attention has been given to its ribosomally encoded antibacterial proteins. Therefore, highlighting the need to investigate their natural occurrence and explore their potential role as an antimicrobial agent. In this study, we investigate the distribution of a putative S-pyocinogenic operon designated as Pyocin S9c, in different *Pseudomonas* relative strains using reference sequence obtained from *P. aurantiaca* PB-St2 (Mehnaz et al. 2014). The affiliation of active pyocin S9c to the corresponding gene cluster was confirmed by its heterologous expression in *E. coli*. For primitive functional analysis, experimental evidence was gathered by antimicrobial testing and associated endonuclease activity. To our knowledge, it is the first report demonstrating the active presence of soluble pyocin in general and pyocin S9c in specific from *P. aurantiaca* PB-St2.

Materials and methods

Strains, plasmids and culture methods

Previously characterized strains of *Pseudomonas* species were routinely maintained on King's B medium (King et al. 1954). Other gram-negative and gram-positive bacterial indicator strains were routinely maintained on LB agar (Bertani 2004) at 30–37 °C, according to their optimum growth temperature unless otherwise stated. Liquid cultures were grown in an orbital shaker at 150 rpm. For cloning and expression, pET28a (+) was the choice of vector. Pyocin S9c-Im9c gene-specific cloning primers were designed using the nucleotide sequence of pyocin S (Locus U724_00285; coordinates: 89833–91110) and cognate immunity (Locus U724_00290; coordinates: 91123–91401) genes from the genome of *Pseudomonas chlororaphis* subsp *aurantiaca* PB-St2 (Mehnaz et al. 2014) and analyzed for specificity by NCBI's nucleotide BLAST program. Primers were synthesized by Eurofins, USA (Table 1).

Table 1 Strains, plasmids, and primers used in this study

Strain, Plasmids & Primers	Relevant properties	Source or Reference
Strains		
P. chlororaphis subsp. *aurantiaca* PB-St2	Wild-type strain	Mehnaz et al. (2009)
P. chlororaphis subsp. *aurantiaca* ARS38, FS2, GS1, GS3, GS4, GS6, GS7; *P. chlororaphis* RP4	Wild-type strain/Indicator strain	Shahid et al. (2017)
P. aeruginosa PAi *P. aeruginosa* PAc1-PAc5 [a] *P. fluorescens* PsiRS1 *P. kilonensis* OSRS3 *B. cereus* BCi *S. aureus* Stpi *S. enterica* SLi *K. oxytoca* KO	Indicator strain	This Study, FCCU culture collection
E. coli DH10β	F– mcrA Δ(mrr-hsdRMS-mcrBC) φ80lacZΔM15 ΔlacX74 recA1 endA1 araD139 Δ (ara-leu)7697 galU galK λ– rpsL(StrR) nupG	Thermo Scientific™ cat # EC0 113
E. coli BL21 (DE3) pLysS	Low background expression host *E. coli* B F^{-} dcm ompT hsdS (rB^{-} mB^{-}) gal λ(DE3) [pLysS Cam^{r}]	Novagen cat # 69,451
Plasmids		
pET-28a (+)	Expression plasmid; N-Terminal & C-Terminal His-Tags, kanamycin resistance, T7lac promoter	Sigma-Aldrich cat # 69,864
pET-28a_PysS9c-Im9c	pET-28a(+) containing PyocinS9c operon from PB-St2, at *Hind*III-*Xho*I sites	This Study
pTZ57R/T	Cloning plasmid, linearized and ddT tailed, 2886 bp,	Thermo Scientific cat # K1214
Cloning Primers[b]	**Primer sequence 5´-3´**	
S9cF	AATGGGGAG**AAGCTT**GGATGAGTGGCTACGTC	This Study
S9cR	TTT**CTCGAG**CACCTTAACCCTTGAACCCTGGC	This Study
Sequencing Primers		
T7promoter Universal	TAATACGACTCACTATAGGG	Macrogen
T7terminator Universal	GCTAGTTATTGCTCAGCGG	Macrogen

[a] Clinical isolate identified on biochemical basis [b] The bold sequences in primer fragments indicate restriction enzyme's recognition sites with underlined bases manipulated in primer sequence against the target gene sequence. The red-colored sequence at the 5'-end of the primers was added as an overhang for optimal enzyme activity. The forward primer was designed to be in frame with an N-terminal histidine fusion tag

Phenotypic screening of bacteriocinogeny in *P. aurantiaca* PB-St2

The bacteriocin production in *P. chlororaphis* subsp. aurantiaca PB-St2 was assessed using the double agar diffusion method with modifications (Blasco et al. 2023). The test strain of PB-St2 was grown overnight in LB broth, diluted to an OD_{600} of 0.5 and treated with or without mitomycin C (MMC 0.5 µg/ml; Abcam #ab120797) for 6 h. The MMC as DNA damage inducer was used to test production of pyocins under SOS response. Standard inoculum of MMC induced and un-induced test culture (10^8 CFU/ml) was prepared and spot inoculated on LB agar followed by incubation at 30 °C for 24 h. The bacterial growth was removed and residual cells were killed by flooding the culture plate with 10 ml chloroform for 30 min. Later, chloroform was decanted and plates were allowed to air dry by evaporation. Then, indicator bacterial strains were seeded in 0.7% soft LB agar at 0.4% concentration. And overlaid on test culture plates. These plates were then incubated at 30–37 °C according to the indicator's optimum growth temperature. The choice of indicators to test pyocin-based antibiosis included seventeen strains belonging to 5 different but closely related Pseudomonas species and four distant bacterial genera as internal inhibition control (Table 1). Additionally, *P. aurantiaca* PB-St2 was used both as a producer and an indicator strain in a self-inhibition control. The bacteriocinogeny was tested positive on the appearance of a clear zone around the test spot. The experiment was conducted in triplicates for each indicator strain.

Bioinformatic analysis of pyocin S9c

The in-silico computation analysis was performed for identification of critical structural component of target protein and to make informed choices for its purification and functional characterization. Hence, primarily the sequence and structure-based homology was performed for the functional annotation of candidate putative Pyocin S systems from *P. chlororaphis* subsp. *aurantiaca* PB-St2. Using InterPro DB (Blum et al. 2020; https://www.ebi.ac.uk/interpro/), the amino acid sequence was analyzed for conserved protein domains, signature elements and motifs. The target system was subjected to structural modeling using the protein threading (Fold recognition) method. This approach allowed the comparison of the target protein with homologous proteins having known or solved structures available in PDB. Three-dimensional structure and constituent domain boundaries were attained with the highest-scoring protein templates in PDB using the I-TASSER MTD server (https://zhanggroup.org/I-TASSER-MTD/). Structure visu alization was performed with PyMOL (www.pymol.org).

Sequence-based protein localization was predicted using several webservers (SignalP 6.0, SOSUI, MemBrain 3.0, and TOPCON).

Molecular screening and phylogenetic analysis of pyocin S9c

To determine the distribution of target gene among closely related *Pseudomonas* species, genotypic screening of S9c was conducted by PCR analysis. Initially DNA was isolated from all *Pseudomonas* strains using GeneJET™ Genomic DNA purification kit (Thermo Scientific™ # K0722, USA), as per instructions. Initially, the PCR profile was optimized using *P. aurantiaca* PB-St2 as a reference strain. Gradient PCR was performed at 6 different annealing temperatures i.e., 55, 57, 59, 61, 63 and 65 °C in gradient thermocycler (Applied Biosystem; Veriti™96 Well Thermal Cycler; Model Number 9902) along with a positive control of 16 S rRNA gene at 55 °C. The reaction mixture was prepared using High-fidelity Phusion PCR mix (Thermo Scientific™ # F548S, USA) according to the manufacturer's instructions. PCR profile included an initial denaturation for1 min at 98 °C, 30 cycles of denaturation for 1 min at 98 °C, annealing at the above mentioned 6 different temperatures for 5 s, extension for 20 s at 72 °C, final extension for 1 min at 72 °C and storage for 5 min at 4 °C. The PCR protocol with optimized annealing temperature was later employed to screen genomes of 16 closely related *Pseudomonas* strains. PCR samples were analyzed on 1% agarose gel in a gel documentation system (UVP Gel Doc-It™ 310 Imaging System. P/N 97-0266-02; S/N A050311-004. 260 V–50 Hz). Target amplicons were gel purified using the GeneJET™ Gel Extraction kit (ThermoScientific™#K0691, USA) and sent for sequencing with both forward and reverse gene-specific primers to Macrogen Inc. (Korea). Sequence reads were manually trimmed to remove low-quality data and consensus sequences were generated using the Cap contig assembly program in Bioedit sequence alignment editor (ver 7.2.5). The assembled sequences were searched for homology on the NCBI nucleotide BLAST program and submitted to NCBI's GenBank database for accession numbers. Molecular phylogeny was analyzed to assess evolutionary divergence of target protein sequence from pre-characterized Pyocin S *DNase* subfamilies S1, S2, S3, AP41, S8, S9 and putative S9-like homologs. Similarly, the distribution and evolutionary distance of pyocin S9c subtype among relative species of *Pseudomonas chlororaphis* group were also analyzed by comparing the protein sequences from closest relatives retrieved from NCBI protein Database. Multiple sequence alignment (MSA) was performed by Clustal X program and phylogenetic trees were constructed by the Maximum Likelihood (ML) method using MEGA11 software. The tree output was visualized and annotated using the iTOL server (Letunic and Bork 2024; https://itol.embl.de).

Plasmid construction pET28a-PysS9c-ImS9c

Cloning of Pyocin S9c-Im9c operon was performed in pET28a expression vector to facilitate downstream target protein purification. The PCR amplicons from PB-St2 were sequentially double digested with HindIII/XhoI, gel purified, and then ligated into the corresponding sites of pre-digested *E. coli* expression vector pET28a (+) using T4 DNA ligase to give *pET28a* -PysS9c-Im9c (Table S2b). The expression cassette was in-frame with an N-terminal His_6 fusion tag. The ligation mixture was electroporated in *E. coli* DH10B competent cells. Colony PCR was performed to screen positive clones containing genes of interest. Plasmids were isolated from the PCR-positive colonies using GeneJET Plasmid minprep kit (Thermo Scientific™ cat # K0502, USA) and cross-verified by double digestion with HimdIII/XhoI (Table S2c). For final confirmation, plasmids were sent for sequencing to Macrogen Inc (Korea), with plasmid and gene-specific primers (Table 1) ensuring complete coverage of genes of interest.

Expression and immuno-blot detection of pyocin S9c

In order to identify the expression of target protein from transformed *E. coli* host The Sequence verified plasmid was transformed in *E. coli* expression host BL21 (DE3 pLysS) using LB agar supplemented with kanamycin (kana, 100 μgml^{-1}) and chloramphenicol (cm, 50 μgml^{-1}). The optical density of the transformed bacterial culture was monitored periodically. At an $O.D_{600}$ of 0.6–0.8, culture was induced with 0.25, 0.5, and 1 mmol/l Isopropyl β-D-1-thiogalactopyranoside IPTG (Sigma life science, lot#107M4032V) at 28 °C for 8 h. After incubation, cells were harvested and re-suspended in Tris-buffered saline (TBS: 50 mM Tris, 250 mM NaCl pH = 7.5, 5% glycerol & 1 mM PMSF). Cells were lysed using an ultrasonic cell disruptor (Sonics Vibra cell, KS-250 F Madell Technology Corp. USA) for 20-sec pulses: 10 s rest in 20 cycles. The total cell lysate was centrifuged at 14,000 rpm for 30 min at 4 °C, and the supernatant was then filtered through a 0.22 µm membrane to remove any residual cell debris. The cell-free lysate from IPTG-induced and un-induced (control) was run in duplicate on 12% SDS-PAGE to assess the expression of pyocin S9c. The gel was stained with Coomassie blue R-250 (BDH Laboratory, # 44328-3 M). The expected size of the target protein was compared to PageRuler™ Pre-stained Protein Ladder (Thermo Scientific™ cat

26616). To affirm the successful expressionFor immunoblot analysis, sample proteins were transferred from SDS-PAGE on a methanol-activated PVDF membrane at 20 V for 60 min using a Tans-Blot SD Semi-Dry Transfer Cell (Bio-Rad). The membrane was washed twice with TBST buffer (1X) for 5 min, before and after blocking it for 15 min with freshly prepared 5% BSA solution. The membrane was then treated overnight with Anti-6xHis Tag mouse IgG1 MAb (1:3000, cat # D191001), followed by 1-hour incubation in HRP-conjugated Goat anti-mouse IgG (1:5000, cat # D110087) secondary antibody (IBBI Sangon Biotech, Shanghai) with shaking incubation at 4 °C. Following the manufacturer's instruction, the blot was developed using the Western Blot Amplification Module (Bio-Rad, cat # 170–8230, USA) and Opti-4CN substrate kit (cat # 170–8235). The Trans-Blot was then observed for his-tagged signal and processed for imaging (BioRad Molecular Imager ChemiDoc ™ XRS + system; Bio-Rad software: Image Lab 5.2.1).

Purification and tandem mass spectrometry of pyocin S9c

The purification of PysS9c was conducted from a production culture of 4 L. The cells were harvested (HERMLE labortechnik GmbH, Type: Z 513 K, SN 35130017, Germany) and resuspended in 1X TBS containing 20 mM imidazole (pH 7.4). The cell-free lysate was prepared as mentioned earlier. PysS9c protein was purified through Akta fast protein liquid chromatography (FPLC) (GE Healthcare) on 5 ml HisTrap ™ FF column (Ni-NTA column, GE Healthcare, USA), pre-equilibrated in the buffer same as the sample buffer. The bound proteins were eluted on an imidazole gradient ranging from 10 to 500 mM over 2 column volumes. Fractions were analyzed on SDS-PAGE. Target protein fractions were pooled and dialyzed overnight in TBS buffer at 4 °C. Further purification was performed by size-exclusion chromatography SEC superdex 200 increase (GE Healthcare, USA) by isocratic elution in TBS buffer. Five milliliters of HiTrap™ column (GE Healthcare, USA), was employed to desalt. Finally, the protein was eluted in the same buffer. The concentration of purified protein was estimated by A280 nm using the sequence-based extinction coefficient ε280, 52,620 M^{-1} cm^{-1}(ExPASy ProtParam). The purified protein band was excised and outsourced for identification by tandem mass spectrometry (KAUST Core Labs, Saudia Arabia). Data analysis was performed with Sequest HT (v1.17); XCorr:2.98. The fragment match tolerance was set to 0.6 Da and -H_2O; y; -NH_3; y; -H_2O; b; -NH_3; b fragments were used for search.

Sensitivity testing of pyocin S9c

The antimicrobial activity of purified pyocin S9c was evaluated following the disc diffusion method (Paškevičius et al. 2022) with some modifications. The bacterial strains for susceptibility testing were selected based on the absence of the pyocin S9c system and the susceptibility to crude bacteriocins of PB-St2. Strains were seeded on Muller-Hinton agar by pour plate method using 0.1% of standard bacterial inoculum (1.5×10^7 CFU/ml). A stock solution of 100 µg/ml of purified protein was two-fold diluted and 10 µl of each dilution was applied on sterile discs pre-transferred on seeded plates. Plates were then incubated for 24 h at the optimum growth temperature of each strain and scored for minimum inhibition concentration (MIC).

Endonuclease activity by plasmid nicking assay

The endonuclease activity of purified S9c was preliminary tested on qualitative scale with genomic DNA substrate from susceptible host strain to establish the cleavage trend for target catalytic protein. In addition, purified pyocin S9c was quantitatively assessed for its endonuclease activity using 0.35 µg of pTZ57R plasmid as a substrate in this plasmid nicking assay. The assay was performed at 37 °C in 50 mM Tris-Cl buffer (pH 7.5) in a final volume of 50 µl. Two independent reactions were set up to determine the impact of selected bivalent metal ions on in-vitro DNase activity. The reactions were initiated by adding pyocin S9c to a final conc of 0.2 µM in the presence of 10 mM Mg^{+2} or Mn^{+2} ions. Small aliquots of 10 ul were withdrawn from the reaction mix at different time points 5, 10, 15, and 20 min, and treated with gel loading dye, containing 60 mM EDTA. The integrity of plasmid isoforms was compared between control and pyocin-treated samples supplemented with tested metal ions, on 1% agarose gel. A densitometric quantification of supercoiled and open-circular forms of pTZ57R plasmid was performed using Image J 1.54.

Results

Bacteriocin production

The phenotypic assay demonstrates the bacteriocinogenic potential of *P. aurantiaca* PB-St2 against closely related *Pseudomonas* species (Fig. S1 a) during the log phase of growth in contrast to the non-inhibition of distant bacterial genera (data not shown). The diffusible antimicrobials of PB-St2 were active against *P. aeruginosa* PAi, PAc3, PAc4 and P. *fluorescens* Psi-RS1 as indicated by wide to moderate sized inhibition zones extending beyond the bacterial

growth. In addition, indicators PAi showed the highest sensitivity only under un-induced conditions. In contrast, PsiRS1 was equally sensitive with or without MMC induction (Fig. 1). Conversely, no inhibition was recorded against *P. aeruginosa* PAc2, PAc5, and other gram-positive and negative indicator strains used (Table 1). In the case of *P. aeruginosa* PAc3 and *P. kiloensis* OSRS3, restricted inhibition was observed only under MMC induction by PB-St2 antimicrobials, which might be due to presence of high molecular weight tailocins or lower sensitivity of indicator strains to any soluble pyocin under tested conditions.

Sequence analysis and structure modeling

The putative pyocin S clusters were mined from the genome sequence of *P. chlororaphis* subsp. *aurantiaca* PB-St2 (Table S1). The functional annotation of the target Pyocin S protein sequence was performed by classifying it into homologous protein families based on the presence of conserved domains or sequence motifs as depicted in Fig. 2a. Like related DNase-type I pyocin S, selected pyocin S from PB-St2 was assumed to be synthesized as a binary protein complex encompassing a multidomain cytotoxic protein with 425 amino acids and a cognate immunity protein with 92 amino acids. The N-terminal domain was annotated as an un-integrated feature due to the absence of any amino acid sequence similarity with characterized HNH-dependent pyocin S DNases.

The interPro DB output showed a conserved translocation pyocin S domain from 161 to 292 residues and an endonuclease domain with an HNH motif at the C-terminal of the protein. The sequence boundaries of PysS9c predicted by I-TASSER-MTD, were used in the pairwise alignment of respective domains with reference domains of pre-characterized DNase-type colicins and pyocins. In pairwise comparison, the translocation domain showed sequence conservation ranging from 26 to 80% while the C-terminal cytotoxic domain showed 44–53% similarity with other DNase-type pyocins. However, the highest similarity was observed with the DNase domain of S9-like pyocin from *P. prosekii* CCM 8881. The cognate immunity protein Im9c revealed 52% similarity with the immunity protein of pyocin AP41 system and 41–43% identity with the related HNH-type pyocin S system. The first immunity gene im9c is followed by a second immunity gene im9c2 that is also similar to related colicin E7 (i. 57%; c. 98%) and pyocin S2 immunity proteins (i. 52%; c.98%). Pyocin S9c is more closely associated with Pys S9a and S9b isoforms from the same strain PB-St2 in amino acid sequence conservation and the presence of a conserved HNH motif. However, the fourth pyocin S domain-containing protein from PB-St2 named pyocin Sd showed no similarity with the N and C-terminal domains of pyocin S9c. Sequence homology identified 53% similarity of pyocin Sd C-terminal domain with pyocin S3 and 51% with pyocin Sn. Thus, pyocin Sd was predicted to be a non-HNH pyocin S3-like DNase protein. All three S9 (a, b & c) and the fourth Sd/S3-like subtypes were commonly found in several strains of *P. chlororaphis* subspecies.

The 3-dimensional model of pyocin S9c killing domain KD was curated using the I-TASSER server. The structural similarity with colicin E9 KD can be seen in Fig. 2b (I), for which the crystal structure had been solved (Klein et al. 2016). Based on sequence and structural homology, pyocin S9c should have an affinity with DNA substrate and bivalent metal cations as possible binding ligands. The essential residues involved in ligand binding are 2, 47,48,51,80,81,95,9

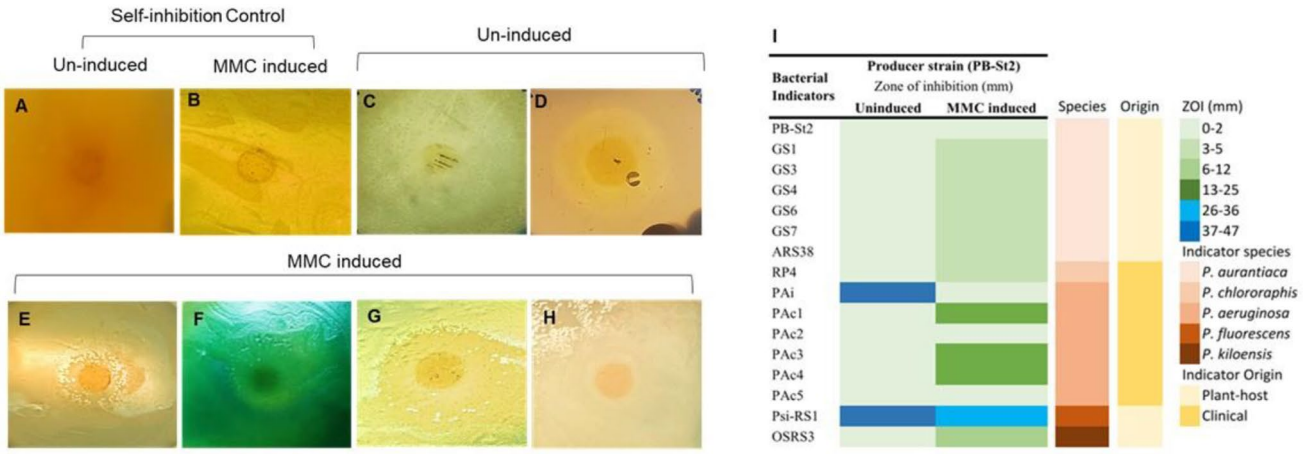

Fig. 1 Phenotypic screening of bacteriocinogeny in *P. chlororaphis* subsp. *aurantiaca* PB-St2 against closely related Pseudomonas species. **a**+**b** PB-St2 tested for self-inhibition with or without MMC induction; **c**+**d** inhibition of *P. aeruginosa* PAi and *P. fluorescens* Psi-RS1 by PB-St2 without induction; **e-h** from left to right, the inhibition of PAc3, PAc1, PAc4, and OSRS3 by PB-St2 with MMC induction; **i** Heatmap depicting pyocin based antibacterial activity against five Pseudomonas specie relatives. The bacterial indicators included strains of both clinical and plant-associated origin

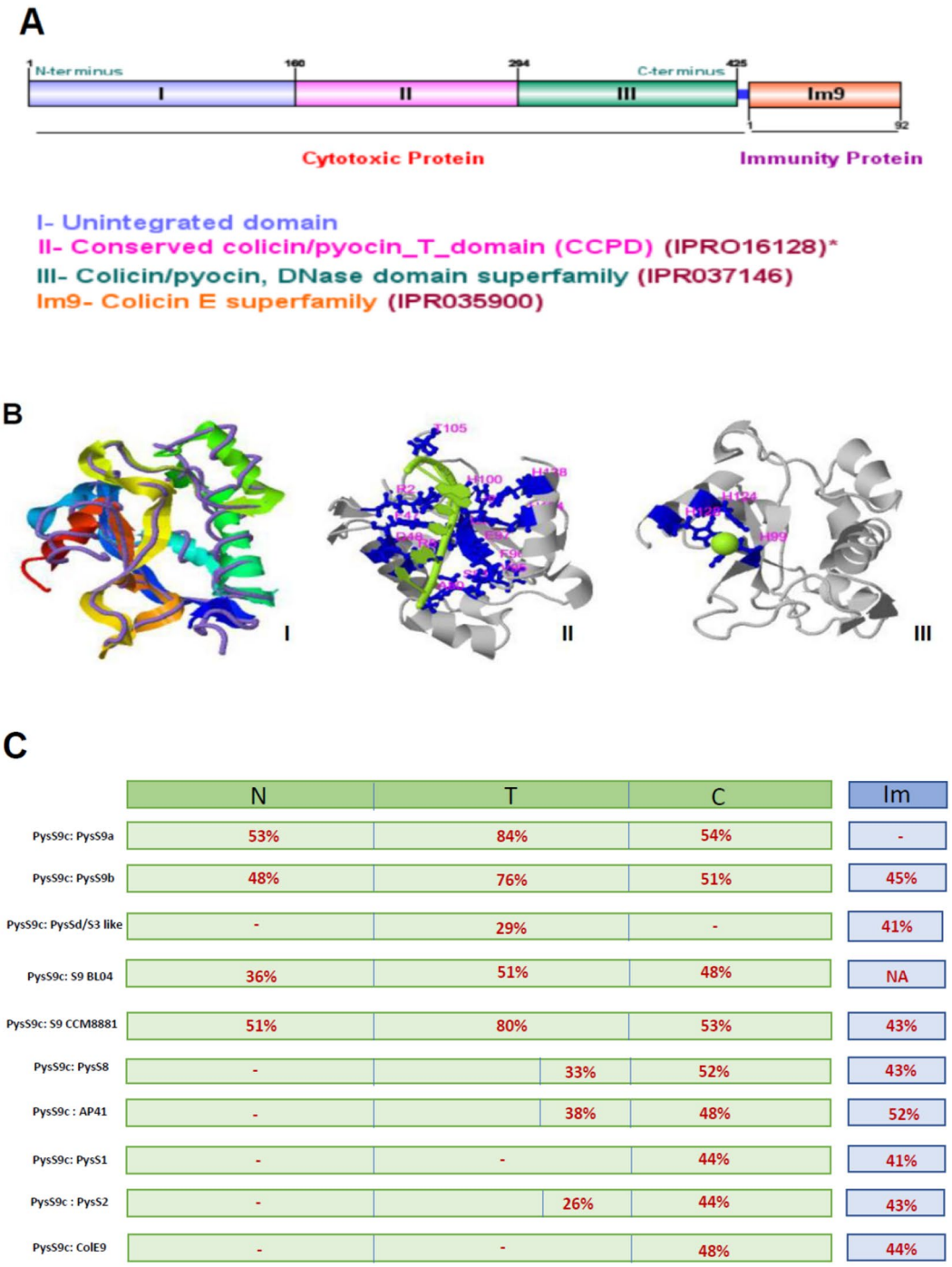

Fig. 2 **a** Schematic diagram of proposed pyocin S9c multi-domain architecture from *P. aurantiaca* PB-St2 with proposed domain boundaries (**I-TASSER-MTD**), conserved domains, functional motifs and sites (*indicates Interpro database identifier of homologous protein domain/family). The schematic illustration was created using DOG 2.0 protein domain structure illustrator. **b** Homology modeling of Pyocin S9c DNase domain from (I) Structure model of PyocinS9c (killing domain, KD) is shown in cartoon representation, superimposed by its closest structural analog Colicin E9 DNase domain (PDB identifier:1FSJ), depicted as backbone trace (II) Structure-based functional annotation indicated residues contributing to nucleic acid binding affinity; The nucleic acid is shown as the binding ligand in yellow-green while the residues involved in binding are shown in blue sticks (III) Mg+2 specific binding residues for catalytic activity of DNase domain H99, H124, H126 **c** Pairwise comparison of amino acid identities between Pyocin S9c and pre-characterized Pyocin S/Colicin E homologs containing conserved endonuclease (H-N-H) motif. Comparison of pyocin S9c with PysS9a, S9b and Sd/S3-like in PB-St2. Representatives from Pyocin S9 cluster entails putative S9 from *P. aeruginosa* BL04 (Acc. no. SAMN02360717) and characterized S9-like pyocin from *P. prosekii* CCM 8881 (Ga0299921-104634), NA: not identified

6,97,98,99,100,105,124,128 (C-Score = 0.71) as modeled in Fig. 2b (II). The expected side chains involved in predicted Mg + 2 activated catalysis are H99, H124, and H128 as evident in Fig. 2b (III).

Molecular screening and phylogenetic analysis of pyocin S9c

Using *P. chlororaphis* subsp. *aurantiaca* PB-St2 as a reference strain, the designed primers were optimized at an annealing temperature Ta of 55 °C for the amplification of pyocin S9c-immunity operon (1.59 kb) by gradient PCR (Fig. S1c). PCR typing was then conducted on pre-optimized conditions to analyze the distribution of pyocin S9c system among *P. chlororaphis* subsp. *aurantiaca* relative strains and across closely related *Pseudomonas* species. Six out of seven *P. chlororaphis* subsp. *aurantiaca* strains ARS38, FS2, GS1, GS3, GS4, and GS6 and one *P. chlororaphis* strain RP4 were positive for S9c-im9c system except for *P. chlororaphis* subsp. *aurantiaca* GS7 (Fig. 3a). Other closely related *Pseudomonas* species were recorded negative including six strains of *P. aeruginosa* PAi, PAc1-PAc5, and one strain each of *P. kiloensis* OSRS3 and *P. fluorescens* Psi-RS1. The nucleotide identity of the sequenced amplicons from different strains of *P. chlororaphis* subsp. *aurantiaca* i.e., GS3 (Acc. no PP883094); RP4 (Acc. no PP883095); GS4 (Acc. no PP883096); GS6 (Acc. no PP883097); ARS38 (Acc. no PP883098); FS2 (Acc. no PP883099); GS1 (Acc. no PP883100) showed 99–100% similarity with the reference sequence from PB-St2. The sequencing read from ARS38 also showed 100% similarity with S9c-im9c system (gene locus: FD951_16490 to FD951_16485) verified in the whole genome sequence of ARS38 (Mehnaz et al. 2020; GenBank # CP045221). Pairwise and multiple sequence alignment of protein sequences were performed to infer the evolutionary distance between related but distinct Pyocin S DNase subtypes. The molecular phylogenic analysis placed pyocin S9c from PB-St2 with its closest S9-like relative from *P. prosekii* CCM8881 along with distant S9 homologs from *P. aeruginosa* BL04 and VRFPAO1, in pyocin S9 clade (Fig. 3b). The PCR screening and gene homology search for pyocin S9c from the NCBI database using Blastp program implied that the S9c amino acid sequence is more conserved in *P. chlororaphis* subsp. *aurantiaca* ARS38, StFRB508, Tre132, K27, M71 (i. 98–100%, c. 99–100%) and *P. aureofaciens* ChPhzS24, 66, 30–84 strains ranging from (i. 87–99%, c. 99–100%). On the other hand, S9c isoform in *P. chlororaphis* subspecie *chlororaphis* showed only 72% similarity while *P. chlororaphis* subspecie *piscium* strains ZJU60, ChPhzS140, ATCC 17,411 had 46–64% identity with a 99% sequence coverage, depicted by the molecular phylogenic analysis (Fig. 3c) However, like any other pyocin subtype, pyocin S9 is also not a species-specific trait. For instance, S9c-like homologs were identified in genomes of other plant-associated fluorescent pseudomonads including strains of *P. cichorii*, *P. brassicacearum* (i. 64%); *P. frederiksbergensis*, *P. nunensis*, *P. syringae*, *P. psychrophila* (i. 63%); *P. prosekii*, *P. savastanoi* (i. 62%); *P. fluorescence P. asplenii*, *P. capsici*, *P. cavernicola* (i. 61%), *P. moraviensis*, *P. allivorans* (i. 60%) *and P. viridiflava*, *P. helmanticensis* (i. 59%) with a sequence coverage of 89–99%. In addition, S9c homologs were also identified in numerous yet unclassified *Pseudomonas* sp. SlBt23, RW409, NFPP07 & MRSN 12,121 strains with 75–91% similarity.

Moreover, *P. aeruginosa* BL04 has an orphan cytotoxic S9 protein without a cognate immunity partner. Similarly, *P. chlororaphis* subsp. *aurantiaca* JD37 showed 94% homology with S9c cytotoxic protein but it lacked the associated immunity partner, which might be due to an incomplete event of horizontal gene transfer. On the other hand, few *P. chlororaphis* subsp. *aurantiaca* strains PCM2210, DSM19603, and M12 had only homologous immunity proteins with 91–92% similarity to Im9c, indicating the ability to protect against related pyocins.

Expression and immuno-blot detection of pyocin S9

The pyocin S9c and its cognate immunity genes (1599 bp) were cloned into a pET28a (+) vector and transformed in *E. coli* DH10β cloning host (Fig. 4 and Fig. S2a). Sequence verified plasmid from positive clone was transformed in *E. coli* BL21 (DE3) pLysS and expressed under the control of a T7 promoter. On reaching an OD of 0.7, samples were withdrawn to test the basal expression of the cloned gene cassette before IPTG induction. Subsequent SDS_PAGE analysis differentially identified a protein band with an apparent molecular weight of 50 kDa (including N-term His Tag and PysS9c 46 kDa) in IPTG-induced samples. The presence of His-tag S9c cytotoxic protein was cross-verified on the immune blot in parallel to SDS-PAGE, using anti-His antibodies (Fig. 5). However, the immunity protein was not differentially detected in the crude soluble fractions. In comparison to the insoluble fraction, lower expression of pyocin S9c was observed in the soluble fraction (Data not shown).

Purification and identification of pyocin S9c

The target protein was expressed in low amounts in soluble fraction under variable expression conditions. Expression of the target protein in both soluble and insoluble fractions was verified on immunoblots (data not shown). A production medium of 4 L was processed for pyocin S9c purification.

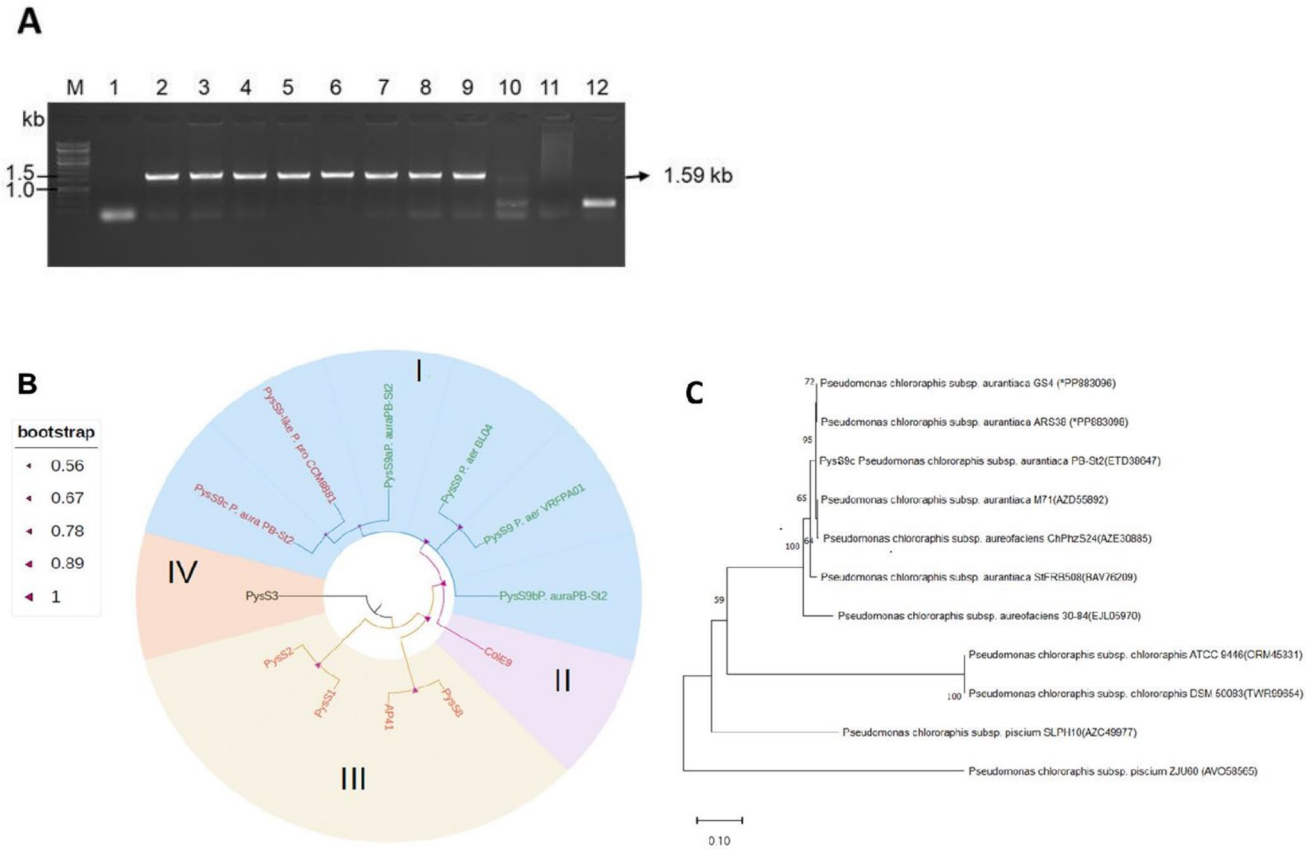

Fig. 3 Detection of pyocin S9c-Im9c amplicons from closely related fluorescent pseudomonads by gel electrophoresis. M: GeneRuler 1 kb DNA Ladder (Thermo Scientific ™ #SM0313, USA); Lane 1: PAi; Lane 2–9: PB-St2, ARS38, FS2, RP4, GS1, GS3, GS4, GS6; Lane 10: GS7, Lane 11: Psi-RS1; Lane 12: OSRS3 **b** Phylogenetic analysis of Pyocin S9c from *P chlororaphis* subsp. *aurantiaca* PB-St2 with characterized and putative HNH-type Pyocin S DN*ases*. An ML phylogenetic tree was constructed using JTT matrix-based model with a bootstrap value of 100 and rooted with Pyocin S3 (non-HNH DNase) from *P. aeruginosa* P12 (Acc. no Q51549), as an outgroup. The predicted HNH-based DNase pyocins of PB-St2, are discriminated by extensions (a), (b), and (c). The characterized pyocin S subtypes are highlighted in red while the predicted ones are in green. I: Pyocin S9 clade, representative species are abbreviated as *P. aura*, *P. chlororaphis* subsp. *aurantiaca; P. aeru*, *P. aeruginosa* BL04 and VRFPA01 and *P. pro*, *Pseudomonas prosekii* CCM 8881. Pyocin S9 cluster entails putative S9 from *P. aeruginosa* BL04 (Acc. no. SAMN02360717), *P. aeruginosa* VRFPA01 (Acc. no KFF32956.1) and characterized S9 from only *P. prosekii* CCM 8881 (JGI, WGS Ac c. no Ga0299921-104634). As for other characterized S9 protein from *P. aeruginosa* UCM B-333 and S9-like homologue from *Pseudomonas* sp. CCM8880, both whole genome and target gene sequences are unavailable, hence excluded from the analysis; II: HNH- DNase E9 from *E. coli* J (Acc. No. B9VM99) from colicin family; III: Characterized Pyocin S HNH-type-I DNases includes PysS1 from *P. aeruginosa* NIH (Acc. No HQ06583); PysS2 from *P. aeruginosa* PAO1 (Acc. no Q06584), AP41 from *P. aeruginosa* PAF (Acc. no Q51502) and pysS8 from P. aeruginosa ET02 (Acc.no A0A1P8L021). The nodes indicate the bootstrap values in the form of arrowheads as provided on the scale (percentage of 100 replicates) **c** Pyocin S9c based phylogeny among relative strains from *Pseudomonas chlororaphis* group by ML method. The tree with the highest log likelihood is displayed. The amino acid sequences of closest relatives were acquired from NCBI's database followed by the accession numbers in brackets. Bootstrap support values with which the closest relatives clustered together are indicated below the branches. The tree is drawn to scale, with branch lengths measured in the number of substitutions per site

During affinity chromatography, both S9c and Im9c were observed in a few lower imidazole fractions on SDS-Polyacrylamide gel with estimated molecular weights of ≈50 and 10 kDA, respectively (Fig. S4). At a higher imidazole concentration of 500 mM, the semi-purified cytotoxic component fused with the N-terminal His tag was separated from its immunity partner. Pooled, de-salted, and concentrated target fractions were further purified by SEC. A protein band with an apparent molecular weight of 50 kDa was verified on Coomassie-stained SDS-PAGE from SEC fractions (Fig. 6a). Following purification, the identity of pure S9c was confirmed by tandem MS analysis. MS2 data showed a sequence coverage of 20% by identification of seven peptides of pyocin S9c. The MS/MS spectrum with the highest spectral counts and significance score, was acquired from the MASCOT server. The identified fragments labeled as b- ions represent the N-terminus while y-ions were derived from the C-terminus of the peptide (Fig. 6c&d).

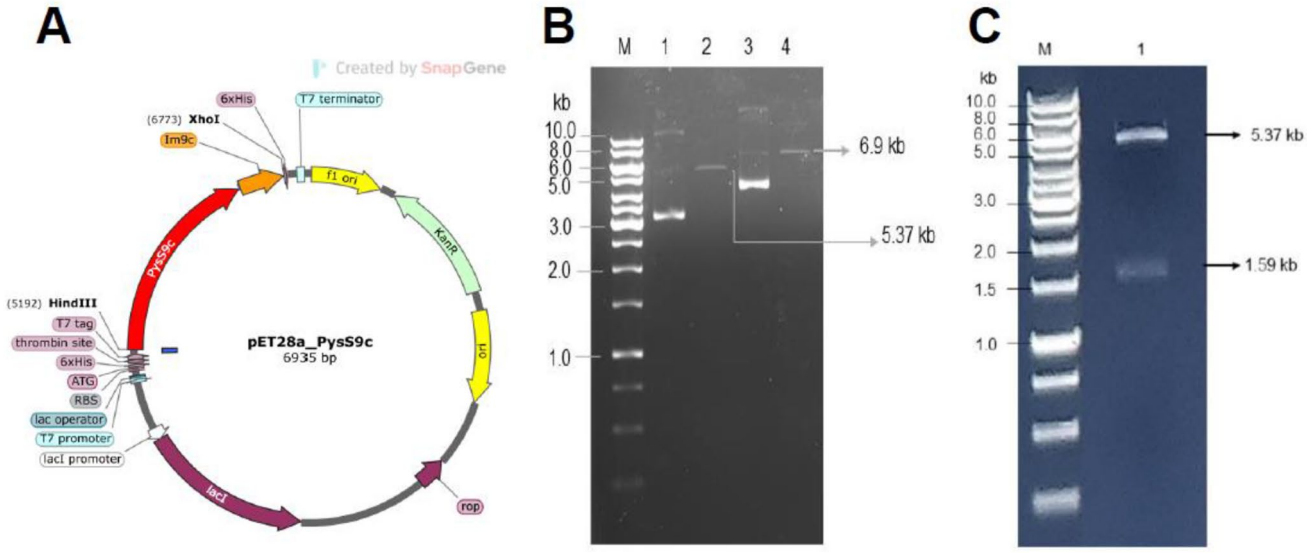

Fig. 4 Development of pET28a-PysS9c-Im expression construct and restriction analysis **(a)** In-silico expression construct designed using SnapGene **(b)** Single Digestion Lane M: GeneRuler 1 kb DNA Ladder (Thermo Scientific ™ #SM0313, USA); Lane 1: un-digested pET28a + plasmid control; Lane 2: pET28a digested with XhoI, Lane 3: un-digested recombinant vector pET28_PysS9-Im9c, Lane 4: pET28_PysS9-Im9c digested with XhoI; **(c)** Double digestion Lane M: GeneRuler 1 kb DNA Ladder; Lane 1: Double digestion of *pET28a*_PysS9-Im9c with HindIII and XhoI

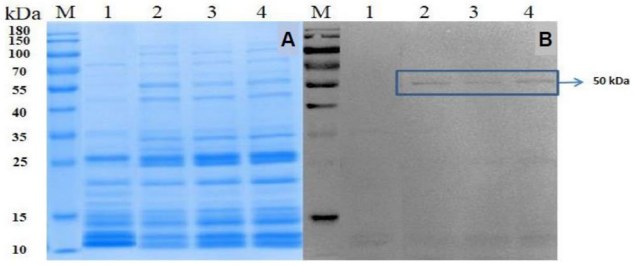

Fig. 5 **a** Identification of soluble recombinant pyocin S9c protein expression on SDS-PAGE **b** Immuno-blot Lane M PageRuler™ Prestained Protein Ladder (Thermo Scientific™# 26616) Lane 1. uninduced *pET28*-PysS9; Lane 2–4: 0.25, 0.5 & 1 mM IPTG induced *pET28*-PysS9. The band corresponding to cytotoxic protein PysS9c is denoted with an arrow

Endonuclease assay

The results of qualitative cleavage of GS7 gDNA shown in Fig. S5 depicted partial cleavage of DNA substrate in 10 min treatment as opposed to complete hydrolysis in 30 min for both tested metal cations. However, the partial cleavage was more pronounced at 10 min interval for Mg^{+2} ions than Mn^{+2} ions. Later, the plasmid nicking assay was performed to quantitatively estimate the cation-dependent endonuclease activity of the purified pyocin S9c cytotoxic protein. Hydrolysis of pTZ57R plasmid DNA was monitored for conversion of supercoiled (SC) forms to open circular (OC) or Linear (L) DNA forms in the presence of Mg + 2 and Mn + 2 ions, on a time scale of 5–20 min (Fig. 7a, b). The gel image was quantitatively analyzed to compute the relative yield of SC and OC isoforms. The L isoform was excluded from the quantification analysis due to the absence of a reference band in control plasmids. Plasmids without S9c cytotoxic protein and respective metal cations were used as controls in computing the relative yield. Higher DNase activity was recorded with Mg + 2 ions within 15 min with complete hydrolysis of DNA substrate. In comparison, plasmids treated with Mn + 2 ions showed a steady trend in hydrolysis of SC to OC and L forms with incomplete hydrolysis over a time scale of 20 min as shown in Fig, 7c. The appearance of both L and OC forms indicates non-specific DNase activity of target protein towards double-stranded and single-stranded DNA molecules.

Discussion

Using classical or recombinant purification methodologies, several S-type (S1-S6, S8, S9, AP41), M-type (PaeM), L-type, and R/F-type pyocins have been characterized from *P. aeruginosa* (Sano 1993; Duport et al. 1995; Nakayama et al. 2000; Joshi et al. 2015). Later, novel pyocins (S7-S12, M4, H-type) were predicted through in-silico analysis of *P. aeruginosa* and other *Pseudomonas* species (Ghequire and De Mot 2014; Sharp et al. 2017). Pyocin effectors differ in genetic architecture, induction cues, cytotoxicity, susceptibility spectrum, and receptor specificity. Recent studies have identified multiple tailocins in *P. chlororaphis* 30–84 (Dorosky et al. 2017, 2018), pyocin S8 from *P. aeruginosa*

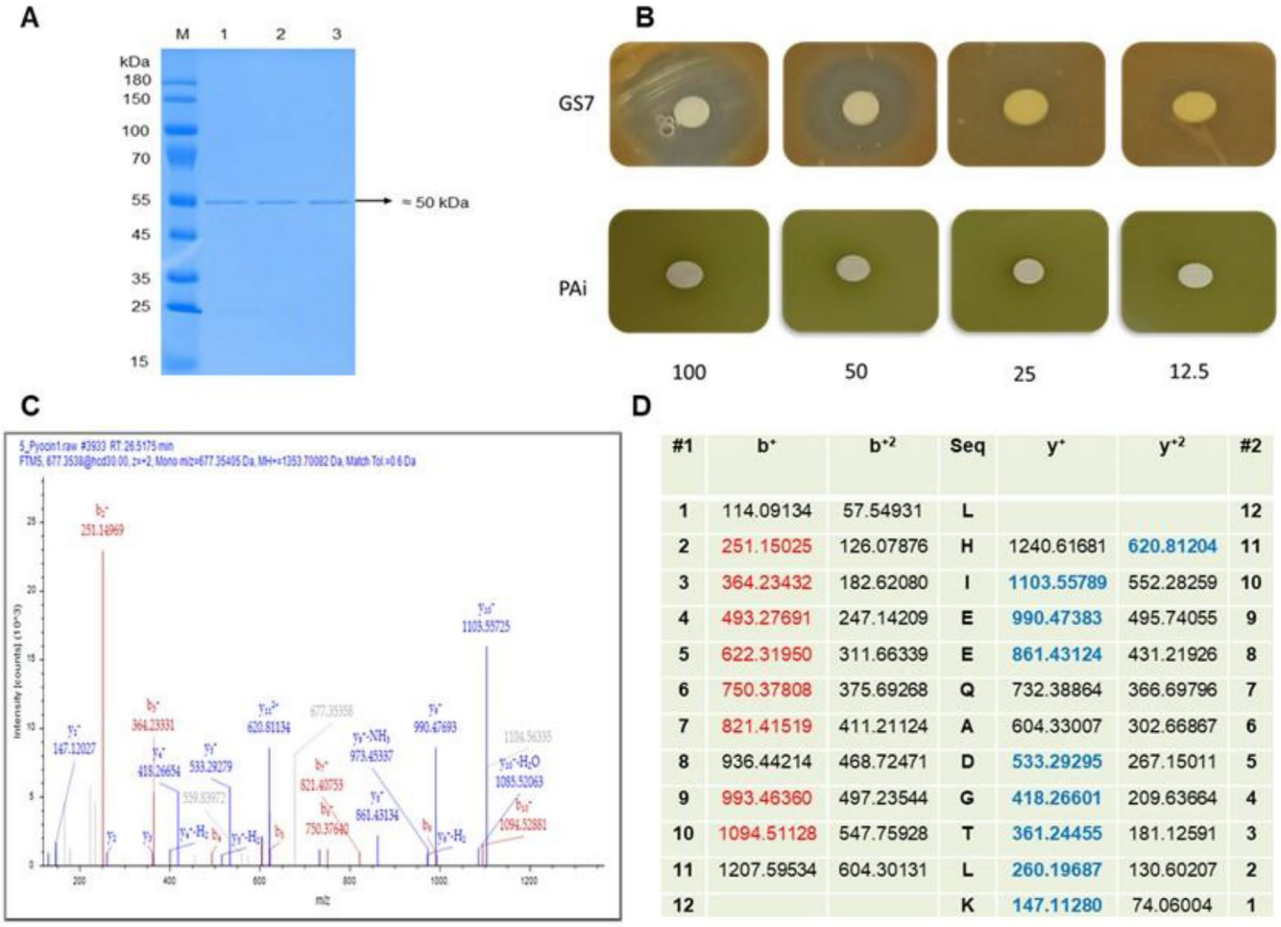

#1	b⁺	b⁺²	Seq	y⁺	y⁺²	#2
1	114.09134	57.54931	L			12
2	251.15025	126.07876	H	1240.61681	620.81204	11
3	364.23432	182.62080	I	1103.55789	552.28259	10
4	493.27691	247.14209	E	990.47383	495.74055	9
5	622.31950	311.66339	E	861.43124	431.21926	8
6	750.37808	375.69268	Q	732.38864	366.69796	7
7	821.41519	411.21124	A	604.33007	302.66867	6
8	936.44214	468.72471	D	533.29295	267.15011	5
9	993.46360	497.23544	G	418.26601	209.63664	4
10	1094.51128	547.75928	T	361.24455	181.12591	3
11	1207.59534	604.30131	L	260.19687	130.60207	2
12			K	147.11280	74.06004	1

Fig. 6 Purification, identification and sensitivity of pyocin S9c **a** SDS-PAGE analysis of purified pyocin S9c cytotoxic protein from Size exclusion chromatographic (SEC) fractions. Lane M PageRuler™ Prestained Protein Ladder (Thermo Scientific™# 26616); Lane 1–3: SEC fractions F3, F4 and F5 **b** In-vitro testing of antimicrobial activity of purified Pyocin S9c against *P. chlororaphis* subsp. *aurantiaca* GS7 and *P. aeruginosa* PAi. The tested inhibitory concentrations were 100, 50, 25 and 12.5 µg/ml with minimum inhibitory concentration (MIC) of 12.5 µg/ml **c** MS/MS spectra of component peptide LHIEEQADGTLK, identified on MASCOT server with the highest significance score of 81 that matched with the reference peptide from Pyocin S9c **d** The masses of identified y- and b- fragments in this sequence are highlighted in blue and red, respectively

ET02 (Turano et al. 2020), and various pyocins in Antarctic *Pseudomonas* strains (Snopkova et al. 2021). In this study, *P. chlororaphis* subsp. *aurantiaca* PB-St2 was screened for pyocin genes, leading to the characterization of Pyocin S9c. This strain encodes three S9-like HNH-type DNases, an S3-like non-HNH DNase, and an R-type tailocin cluster. The bacteriocinogenic potential of PB-St2 was confirmed, showing both narrow and wide inhibition zones against fluorescent Pseudomonads. Diffusible zones may result from soluble determinants, while sharp-edged zones indicate particle-based pyocin activity (Yao et al. 2017). Resistance by distant bacterial genera on bacteriocin production assay supports the identification of pyocins as target antimicrobials.

The production of multiple pyocins from PB-St2 is similar to *P. aeruginosa* PAO1 (S2, S4, S5) (Elfarash et al. 2012) *P. aeruginosa* UCM (S1, S5, S9, Microcin-II-like) strains (Balko et al. 2022). However, presence of multiple S9-like genes suggests intragenomic duplication, a key event contributing to the diversity of pyocin effectors. Thus, even similar pyocin subtypes may exhibit different killing spectra, allowing bacterial strains with diverse antimicrobial effectors to persist effectively in bacterial communities.

Pyocin production is typically triggered by UV irradiation or mitomycin C (MMC), activating RecA to cleave PrtR and induce PrtN-driven transcription (Fernandez et al. 2020). However, PB-St2 exhibited antimicrobial activity against *P. aeruginosa* PAi and *P. fluorescens* PsiRS1 without induction, suggesting a RecA-independent pathway. On the contrary, some pyocins in PB-St2 were only induced under MMC treatment, indicating variability in induction mechanisms. Similar RecA-independent pyocin S9 production was reported in *P. aeruginosa* UCM B-333 (Balko et al. 2022). Another study showed the absence of XerC, a site-specific recombinase may lead to genomic instability and indirectly

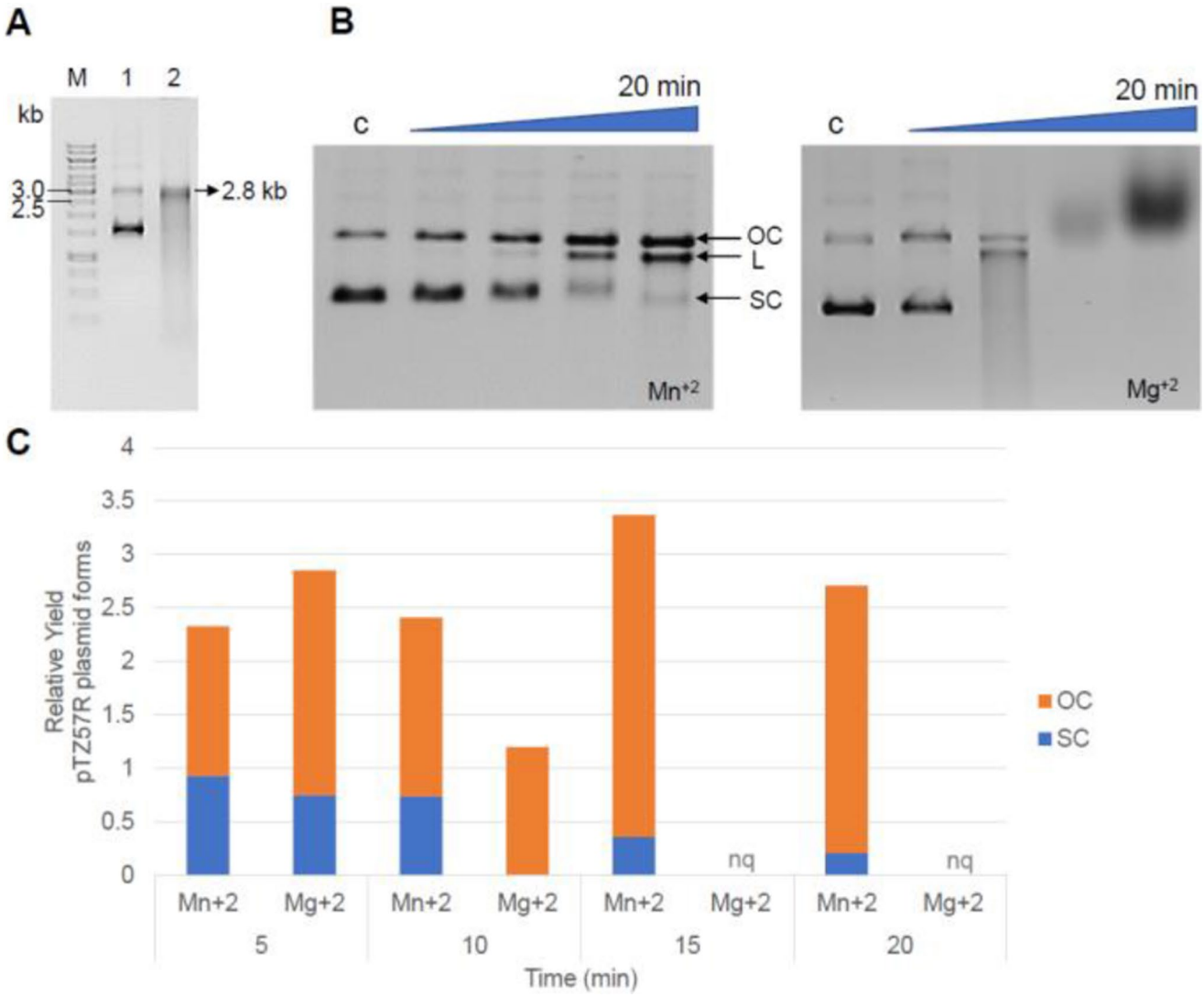

Fig. 7 Plasmid nicking assay analyzed by agarose gel electrophoresis **a** pTZ57R plasmid substrate used in plasmid nicking assay Lane M molecular marker 1 kb Lane 1 undigested pTZ57R Lane 2 pTZ57R digested with HindIII **b** In-gel plasmid nicking activity of Pys S9c under divalent metal ions supplementation, Lane c indicates control sample, OC, L and SC signify open circular, linear and supercoiled plasmid isoforms, respectively **c** Time-scale estimation of endonuclease activity by Pys S9c in plasmid nicking assay. nq: not quantified

stimulating pyocin production by triggering stress responses independent of RecA pathway (Bronson et al. 2022.

The lack of sequence similarity at the N-terminus of S9 cytotoxic proteins suggests distinct receptor-binding specificities, as evident in its specified sensitivity against relative strain of GS7. Hence, the N-terminal and translocation domain diversity contributes to pyocin variation, supporting previous reports (Buth et al. 2018). And by exploiting this diversity, engineered strains with chimeric pyocins and pyocin-colicin effectors were designed by swapping N and C terminus domains to expand their antimicrobial spectrum (Kageyama et al. 1996; Paškevičius et al. 2022).

On the contrary, the cross specie soluble activity observed against *P. fluorescens* Psi-RS1 and *P. aeruginosa* PAi from wild type culture of PB-St2, is a trait commonly associated with L-type pyocins (McCaughey et al. 2014) which are yet unidentified in PBSt2 genome. Likewise, the activity against clinical *P. aeruginosa* strains PAc1, PAc3, and PAc4 suggests the potential of uncharacterized pyocins or tailocins for therapeutic applications. Similarly, *Pseudomonas* sp. CCM 8880, encoding S9-like and Rp4-type tailocins, produced soluble antimicrobials targeting phylogenetically related species. Antarctic *Pseudomonas* sp. CCM 8880 inhibited *P. gregormendelii*, *P. veroni*, *P. mandelii*, and *P. prosekii* but not *P. chlororaphis* sp. *piscium* (Snopkova et al. 2021), which may possess similar S9-like effector-immunity complexes.

Purifying pyocins from wild type strains is often challenging due to its variable expression and secretion mechanisms. Unlike S9 purification from wild-type *P. aeruginosa*

UCM B333 (Balko et al. 2022) or *P. prosekii* CCM 8880 (Snopkova et al. 2021) reporting low native expression, expression of recombinant pyocin S9c under recombinant conditions in *E. coli* was significant to conduct primitive functional characterization. The experimental verification of predicted findings suggests combinatorial significance of bioinformatics and empirical laboratory research.

Given pyocins' role in microbial interactions, PB-St2 distinct pyocin-based antibiosis may prove an effective biocontrol strategy against related phytopathogens. Unlike chemical pesticides, use of characterized biocontrol agents will minimize collateral damage to commensal microflora but also offer an eco-friendly alternative. Furthermore, the sequence diversity in pyocin S9 clusters can be further explored in future to understand their functional significance and receptor specificities for import in susceptible strains.

Conclusion

This study highlights the diverse and complex nature of pyocin production in *Pseudomonas chlororaphis* subsp. *aurantiaca* PB-St2, directed particularly to the profiling of Pyocin S9c. The presence of multiple S9-like genes are expected to provide an evolutionary advantage to this producer strain. *P. chlororaphis* subsp. *aurantiaca* PB-St2 demonstrated narrow spectrum antimicrobial activity against close fluorescent *Pseudomonas* species, reinforcing its bacteriocinogenic potential. The observed antimicrobial activity under both induced and uninduced conditions proposed the possibility of pyocin induction by alternate regulatory mechanism in addition to the widely established RecA-dependent pathway. Moreover, in contrast to the wild type purification methods, the heterologous expression of recombinant Pyocin S9c showed promising results in terms of successful expression of target protein. As a future directive, detailed biophysical characterization and targeted identification of susceptible strains lacking relevant immunity genes and target receptor, will be crucial to assess the full spectrum of the studied protein and similar homologues within and across closely related species. In conclusion, the distinct pyocin-based antibiosis of PB-St2 may offer a promising alternative to chemical pesticides for plant disease control by related phytopathogenic species.

Supplementary Information The online version contains supplementary material available at https://doi.org/10.1007/s00203-025-04345-9.

Acknowledgements Special thanks to Syed Mueez Ali (Forman Christian College, Lahore); Nadezda Levanova, and Mirjam Bardanadt (Dpt. of Pharmaceutical Biology and Biotechnology, Germany) for lab support.

Author contributions M.Z. contributed to the conceptualization of the study, conducted the experimental investigation, performed data curation, formal analysis, and wrote the paper. M.I. provided technical assistance on protein expression and purification. D.N.B. provided technical assistance on construct designing and immune-blot detection. Z.K. provided assistance in data acquisition. A.B. and K.A.M. reviewed manuscript and managed resources. S.M. lead project supervision and administration, editing and critical revision. All authors read and approved the final manuscript.

Funding SM and MZ are highly thankful to the Alexander von Humboldt Foundation (Bonn, Germany) for the Georg Forster Fellowship sponsoring collaboration with German host Dr. Andreas Bechthold. MZ has received research support from the Higher Education Commission (HEC), Pakistan under Indigenous PhD Fellowship Program (Phase-II, Batch-III).

Data availability The whole genome sequence of *P. aurantiaca* PB-St2 is accessible from NCBI GenBank database under the accession # AYUD00000000. Bacterial indicators used in phenotypic assay were identified on the basis of 16S rRNA nucleotide sequences, deposited in NCBI GenBank under following accession IDs: *P. aeruginosa* PAi (OP740518), *P. fluorescens* PsiRS1 (MZ477359), *P. kilonensis* (MZ314341), *B. cereus* BCi (MZ414206), *S. aureus* Stpi (MZ414203), *S. enterica* SLi (MZ414205), *E. coli* ECi (MZ414204). *K. oxytoca* KOi (MZ414202).

Declarations

Ethical approval None required.

Competing interests The authors declare no competing interests.

References

Abbas SR, Shahid I, Javed M, Malik KA, Mehnaz S (2024) Contribution of mineral mobilizing fluorescent pseudomonads in growth promotion of rice (Oryza sativa L.) in nutrient deficient soil. S Afr J Bot 166:88–96. https://doi.org/10.1016/j.sajb.2024.01.023

Abd El-Aziz ZK, El-Sayed MH, Abd El-Ghany AA (2016) Microbial bioremediation of lead by lead-resistant Pseudomonas chlororaphis strain Hel-KE`-14 isolated from industrial wastewater. Int J Pharm Res Allied Sci 5(4):95–107

Balko OB, Zelena LB, Balko OI, Maksymenko LO, Voitsekhovsky VG, Avdeeva LV (2022) Properties of pyocin S9 from *Pseudomonas aeruginosa* UCM B-333. Mikrobiol Z 84(5):48–57. https://doi.org/10.15407/microbiolj84.05.048

Bauer JS, Hauck N, Christof L, Mehnaz S, Gust B, Gross H (2016) The systematic investigation of the quorum sensing system of the biocontrol strain *Pseudomonas chlororaphis* subsp. *Aurantiaca* PB-St2 unveils *auri* to be a biosynthetic origin for 3-oxo Homoserine lactones. PLoS ONE 11:e0167002. https://doi.org/10.1371/journal.pone.0167002

Bertani G (2004) Lysogeny at mid-twentieth century: P1, P2, and other experimental systems. J Bacteriol 186:595–600. https://doi.org/10.1128/jb.186.3.595-600.2004

Blasco L, de Aledo MG, Ortiz-Cartagena C, Blériot I, Pacios O, López M, Fernández-García L, Barrio-Pujante A, Hernández-Garcia M, Cantón R, Tomás M (2023) Study of 32 new phage tail-like bacteriocins (pyocins) from a clinical collection of *Pseudomonas aeruginosa* and of their potential use as typing markers and

antimicrobial agents. Sci Rep 13(1):117. https://doi.org/10.1038/s41598-022-27341-1

Blum M, Chang H, Chuguransky S, Grego T, Kandasaamy S, Mitchell A, Nuka G, Paysan-Lafosse T, Qureshi M, Raj S, Richardson L, Salazar GA, Williams L, Bork P, Bridge A, Gough J, Haft DH, Letunic I, Marchler-Bauer A, Mi H, Natale DA, Necci M, Orengo CA, Pandurangan AP, Rivoire C, Sigrist CJA, Sillitoe I, Thanki N, Thomas PD, Tosatto SCE, Wu CH, Bateman A, Finn RD (2020) The interpro protein families and domains database: 20 years on. Nucleic Acids Res. https://doi.org/10.1093/nar/gkaa977

Bronson AS, Baggett NS, Cabeen MT (2022) DNA damage-inducible pyocin expression is independent of RecA in *xerC*-deleted *Pseudomonas aeruginosa*. Microbiol Spectr 10(4):e0116722. https://doi.org/10.1128/spectrum.01167-22

Buth SA, Shneider MM, Scholl D, Leiman PG (2018) Structure and analysis of R1 and R2 pyocin receptor-binding fibers. Viruses 10(8):427. https://doi.org/10.3390/v10080427

Dingemans J, Ghequire MG, Craggs M, De Mot R, Cornelis P (2016) Identification and functional analysis of a bacteriocin, pyocin S6, with ribonuclease activity from a *Pseudomonas aeruginosa* cystic fibrosis clinical isolate. Microbiologyopen 5(3):413–423. https://doi.org/10.1002/mbo3.339

Dorosky RJ, Yu JM, Pierson LS III, Pierson EA (2017) Pseudomonas chlororaphis produces two distinct R-tailocins that contribute to bacterial competition in biofilms and on roots. Appl Environ Microbiol 83(15):e00706–e00717. https://doi.org/10.1128/AEM.00706-17

Dorosky RJ, Pierson LS, Pierson EA (2018) *Pseudomonas chlororaphis* produces multiple R-tailocin particles that broaden the killing spectrum and contribute to persistence in rhizosphere communities. Appl Environ Microbiol 84:e01230–e01218. https://doi.org/10.1128/AEM.01230-18

Duport C, Baysse Y, Michel-Briand C (1995) Molecular characterization of pyocin S3, a novel S-type pyocin from *Pseudomonas aeruginosa*. J Biol Chem 270(15):8920–8927. https://doi.org/10.1074/jbc.270.15.8920

Elfarash A, Wei Q, Cornelis P (2012) The soluble pyocins S2 and S4 from *Pseudomonas aeruginosa* bind to the same FpvAI receptor. Microbiologyopen 1(3):268–275. https://doi.org/10.1002/mbo3.27

Fang R, Lin J, Yao S et al (2013) Promotion of plant growth, biological control and induced systemic resistance in maize by Pseudomonas aurantiaca JD37. Ann Microbiol 63:1177–1185. https://doi.org/10.1007/s13213-012-0576-7

Fernandez M, Godino A, Príncipe A et al (2020) Characterization of the bacteriocins and the PrtR regulator in a plant-associated Pseudomonas strain. J Biotechnol 307:182–192. https://doi.org/10.1016/j.jbiotec.2019.11.003

Garrido-Sanz D, Arrebola E, Martínez-Granero F, García-Méndez S, Muriel C, Blanco-Romero E, Martín M, Rivilla R, Redondo-Nieto M (2017) Classification of isolates from the *Pseudomonas fluorescens* complex into phylogenomic groups based on group-specific markers. Front Microbiol 8:413. https://doi.org/10.3389/fmicb.2017.00413

Ghequire MGK, De Mot R (2014) Ribosomally encoded antibacterial proteins and peptides from *Pseudomonas*. FEMS Microbiol Rev 38(4):523–568. https://doi.org/10.1111/1574-6976.12079

Ghequire MG, De Mot R (2015) The Tailocin tale: peeling off phage Tails. Trends Microbiol 23:587–590. https://doi.org/10.1016/j.tim.2015.07.011

Hou LL, Kong WL, Wu XQ (2025) Biocontrol activity and action mechanism of Pseudomonas aurantiaca ST-TJ4 against verticillium Dahliae, the causal agent of Acer truncatum wilt. Pestic Biochem Physiol 207:106224. https://doi.org/10.1016/j.pestbp.2024.106224

Jacob F (1954) Biosynthèse induite et mode D'action D'une Pyocine, antibiotique de *Pseudomonas pyocyanea*. Ann Inst Pasteur (Paris) 86:149–160 PMID: 13158940

Jiao Z, Wu N, Hale L, Wu W, Wu D, Guo Y (2013) Characterisation of *Pseudomonas chlororaphis* subsp. *Aurantiaca* strain Pa40 with the ability to control wheat Sharp eyespot disease. Ann Appl Biol 163(2):188–198. https://doi.org/10.1111/aab.12068

Joshi A, Grinter R, Josts I et al (2015) Structures of the ultra-high-affinity protein-protein complexes of pyocins S2 and AP41 and their cognate immunity proteins from *Pseudomonas aeruginosa*. J Mol Biol 427:2852–2866. https://doi.org/10.1016/j.jmb.2015.07.014

Kageyama M, Kobayashi M, Sano Y, Masaki H (1996) Construction and characterization of pyocin-colicin chimeric proteins. J Bacteriol 178(1):103–110. https://doi.org/10.1128/jb.178.1.103-110.1996

King EO, Ward MK, Raney DE (1954) Two simple media for the demonstration of pyocyanin and fluorescin. J Lab Clin Med 44:301–307 PMID: 13184240

Klein A, Wojdyla JA, Joshi A, Josts I, McCaughey LI, Housden NG, Kaminska R, Byron O, Walker D, Kleanthous C (2016) Structural and biophysical analysis of nuclease protein antibiotics. Biochem J 473(18):2799–2812. https://doi.org/10.1128/jb.178.1.103-110.1996

Letunic I, Bork P (2024) Interactive tree of life (iTOL) v6: recent updates to the phylogenetic tree display and annotation tool. Nucleic Acids Res 13:gkae268. https://doi.org/10.1093/nar/gkae268

Ling H, Saeidi N, Rasouliha BH, Chang MW (2010) A predicted S-type pyocin shows bactericidal activity against clinical *Pseudomonas aeruginosa* isolates through membrane damage. FEBS Lett 584(15):3354–3358. https://doi.org/10.1016/j.febslet.2010.06.021

McCaughey LC, Grinter R, Josts I, Roszak AW, Waløen KI, Cogdell RJ, Milner J, Evans T, Kelly S, Tucker NP, Byron O, Smith B, Walker D (2014) Lectin-like bacteriocins from *Pseudomonas* spp. Utilise D-rhamnose containing lipopolysaccharide as a cellular receptor. PLoS Pathog 10(2):e1003898. https://doi.org/10.1371/journal.ppat.1003898

Mehnaz S, Baig DN, Jamil F, Weselowski B, Lazarovits G (2009) Characterization of a phenazine and Hexanoyl Homoserine lactone-producing *Pseudomonas aurantiaca* strain PB-St2, isolated from sugarcane stem. J Microbiol Biotechnol 19:1688–1694. https://doi.org/10.4014/jmb.0904.04022

Mehnaz S, Bauer JS, Gross H (2014) Complete genome sequence of the sugar cane endophyte Pseudomonas aurantiaca PB-St2, a disease-suppressive bacterium with antifungal activity toward the plant pathogen Colletotrichum falcatum. Genome Announc 2(1):e01108–e01113. https://doi.org/10.1128/genomeA.01108-13

Mehnaz S, Bechthold A, Gross H (2020) Draft genome sequence of Pseudomonas chlororaphis subsp. Aurantiaca ARS-38, a bacterial strain with plant growth promotion potential. Microbiol Resour Announc 9(3):e01398–e01319. https://doi.org/10.1128/MRA.01398-19

Michel-Briand Y, Baysse C (2002) The pyocins of Pseudomonas aeruginosa. Biochimie 84(5–6):499–510. https://doi.org/10.1016/s0300-9084(02)01422-0

Morohoshi T, Wang WZ, Suto T, Saito Y, Ito S, Someya N, Ikeda T (2013) Phenazine antibiotic production and antifungal activity are regulated by multiple quorum-sensing systems in *Pseudomonas chlororaphis* subsp. *Aurantiaca* StFRB508. J Biosci Bioeng 116:580–584. https://doi.org/10.1016/j.jbiosc.2013.04.022

Nakayama K, Takashima K, Ishihara H, Shinomiya T, Kageyama M, Kanaya S, Ohnishi M, Murata T, Mori H, Hayashi T (2002) The R-type pyocin of Pseudomonas aeruginosa is related to P2 phage, and the F-type is related to lambda phage. Mol Microbiol

38(2):213–231. https://onlinelibrary.wiley.com/doi/10.1046/j.1365-2958.2000.02135.x

Nowak-Thompson B, Hammer PE, Hill DS, Stafford J, Torkewitz N, Gaffney TD, Lam ST, Molnár I, Ligon JM (2003) 2,5-Dialkylresorcinol biosynthesis in *Pseudomonas aurantiaca*: novel head-to-head condensation of two fatty acid-derived precursors. J Bacteriol 185:860–869. https://doi.org/10.1128/JB.185.3.860-869.2003

Paškevičius Š, Dapkutė V, Misiūnas A, Balzaris M, Thommes P, Sattar A, Gleba Y, Ražanskienė A (2022) Chimeric bacteriocin S5-PmnH engineered by domain swapping efficiently controls Pseudomonas aeruginosa infection in murine keratitis and lung models. Sci Rep 12(1):5865. https://doi.org/10.1038/s41598-022-09865-8

Peix A, Valverde A, Rivas R, Igual JM, Ramírez-Bahena MH, Mateos PF, Santa-Regina I, Rodríguez-Barrueco C, Martínez-Molina E, Velázquez E (2007) Reclassification of Pseudomonas aurantiaca as a synonym of Pseudomonas chlororaphis And proposal of three subspecies, P. chlororaphis subsp. chlororaphis subsp. Nov., P. chlororaphis subsp. Aureofaciens subsp. Nov., comb. Nov. And P. chlororaphis subsp. aurantiaca subsp. Nov., comb. Nov. Int J Syst Evol Microbiol 57:1286–1290. https://doi.org/10.1099/ijs.0.64621-0

Raio A, Puopolo G, Cimmino A, Danti R, Della Rocca G, Evidente A (2011) Biocontrol of Cypress canker by the phenazine producer *Pseudomonas chlororaphis* subsp. *Aureofaciens* strain M71. Biol Control 58:133–138. https://doi.org/10.1016/j.biocontrol.2011.04.012

Rosas SB, Avanzini G, Carlier E, Pasluosta C, Pastor N, Rovera M (2009) Root colonization and growth promotion of wheat and maize by Pseudomonas aurantiaca SR1. Soil Biol Biochem 41(9):1802–1806. https://doi.org/10.1016/j.soilbio.2008.10.009

Sano Y (1993) The inherent DNase of pyocin AP41 causes breakdown of chromosomal DNA. J Bacteriol 175(3):912–915. https://doi.org/10.1128/jb.175.3.912-915.1993

Sano Y, Kageyama M (1981) Purification and properties of an S-type pyocin, pyocin AP41. J Bacteriol 146(2):733–739. https://doi.org/10.1128/jb.146.2.733-739.1981

Sano Y, Matsui H, Kobayashi M, Kageyama M (1993) Molecular structures and functions of pyocins S1 and S2 in *Pseudomonas aeruginosa*. J Bacteriol 175(10):2907–2916. https://doi.org/10.1128/jb.175.10.2907-2916.1993

Shahid I, Rizwan M, Baig DN et al (2017) Secondary metabolites production and plant growth promotion by Pseudomonas chlororaphis and P. aurantiaca strains isolated from Cactus, cotton, and Para grass. J Microbiol Biotechnol 27(3):480–491. https://doi.org/10.4014/jmb.1601.01021

Shahid I, Han J, Hardie D et al (2021) Profiling of antimicrobial metabolites of plant growth promoting Pseudomonas spp. Isolated from different plant hosts. 3 Biotech 11:48. https://doi.org/10.1007/s13205-020-02585-8

Sharp C, Bray J, Housden NG, Maiden MCJ, Kleanthous C (2017) Diversity and distribution of nuclease bacteriocins in bacterial genomes revealed using hidden Markov models. PLoS Comput Biol 13(7):e1005652. https://doi.org/10.1371/journal.pcbi.1005652

Snopkova K, Dufkova K, Chamrad I, Lenobel R, Čejkova D, Kosina M, Hrala M, Hola V, Sedláček I, Šmajs D (2021) Pyocin-mediated antagonistic interactions in Pseudomonas spp. Isolated in James Ross Island, Antarctica. Environ Microbiol 00(00):00–00. https://doi.org/10.1111/1462-2920.15809

Turano H, Gomez F, Domingos RM et al (2020) Molecular structure and functional analysis of Pyocin S8 from Pseudomonas aeruginosa. J Bacteriol 2020:e00346-20. https://doi.org/10.1128/JB.00346-20

Yao GW, Duarte I, Le TT, Carmody L, LiPuma JJ, Young R, Gonzalez CF (2017) A Broad-Host-Range Tailocin from Burkholderia cenocepacia. Appl Environ Microbiol 83(10):e03414–e03416. https://doi.org/10.1128/AEM.03414-16

Zhang Y, Kong WL, Wu XQ, Li PS (2022) Inhibitory effects of phenazine compounds and volatile organic compounds produced by *Pseudomonas aurantiaca* ST-TJ4 against *Phytophthora cinnamomi*. Phytopathology 112(9):1867–1876. https://doi.org/10.1094/PHYTO-10-21-0442-R